PI3K-p110α mediates the oncogenic activity induced by loss of the novel tumor suppressor PI3K-p85α

Lauren M. Thorpe[a,b,c,1], Jennifer M. Spangle[a,b,1], Carolynn E. Ohlson[a,b], Hailing Cheng[a,b], Thomas M. Roberts[a,b], Lewis C. Cantley[d,2], and Jean J. Zhao[a,b,2]

[a]Department of Cancer Biology, Dana-Farber Cancer Institute, Boston, MA 02115; [b]Department of Biological Chemistry and Molecular Pharmacology, Harvard Medical School, Boston, MA 02115; [c]Program in Virology, Harvard Medical School, Boston, MA 02115; and [d]Weill Cornell Medical Center, New York, NY 10065

Contributed by Lewis C. Cantley, May 26, 2017 (sent for review March 21, 2017; reviewed by Ji Luo and Peter K. Vogt)

Mutation or loss of the p85 regulatory subunit of phosphatidylinositol 3-kinase (PI3K) is emerging as a transforming factor in cancer, but the mechanism of transformation has been controversial. Here we find that hemizygous deletion of the *PIK3R1* gene encoding p85α is a frequent event in breast cancer, with *PIK3R1* expression significantly reduced in breast tumors. *PIK3R1* knockdown transforms human mammary epithelial cells, and genetic ablation of *Pik3r1* accelerates a mouse model of HER2/neu-driven breast cancer. We demonstrate that partial loss of p85α increases the amount of p110α–p85 heterodimers bound to active receptors, augmenting PI3K signaling and oncogenic transformation. Pan-PI3K and p110α-selective pharmacological inhibition effectively blocks transformation driven by partial p85α loss both in vitro and in vivo. Together, our data suggest that p85α plays a tumor-suppressive role in transformation, and suggest that p110α-selective therapeutics may be effective in the treatment of breast cancer patients with *PIK3R1* loss.

PI3K | p85 | breast cancer | targeted therapy

Phosphatidylinositol 3-kinases (PI3Ks) are critical coordinators of the cellular response to extracellular signals. Of these, class IA PI3Ks are heterodimeric enzymes containing a p110 catalytic and a p85 regulatory subunit (1). The genes *PIK3CA*, *PIK3CB*, and *PIK3CD*, respectively, encode p110α, p110β, and p110δ, and *PIK3R1*, *PIK3R2*, and *PIK3R3*, respectively, encode the regulatory isoforms p85α, p85β, and p55γ. In the absence of activating signals, the interaction between p85 and p110 stabilizes and inhibits p110 catalytic activity (2). In the presence of growth factors or other signals, ligand binding to receptor tyrosine kinases (RTKs) promotes receptor activation. The p85 subunit binds to activated RTKs, recruiting p110 to the plasma membrane, where a conformational change induced by binding relieves inhibition of p110 catalytic activity.

PI3K pathway hyperactivation is one of the most frequent events in human cancers, commonly resulting from activating PIK3CA mutations, RTK mutation or amplification, or loss of the PI3K antagonist PTEN (3). The contribution of the regulatory isoforms to tumorigenesis has only recently been considered. Somatic mutations in *PIK3R1* have been reported in glioblastoma and endometrial cancer, most of which are substitutions or indels in the iSH2 domain of p85α that contacts p110 (4). These mutants typically bind and stabilize p110, but cannot inhibit p110 catalytic activity (5).

Accumulating evidence also suggests that changes in p85α levels can modulate PI3K activation. In mice, partial loss of p85 isoforms improves insulin sensitivity (6). In some tissues, p85 is present in excess of p110, and monomeric free p85 may act as a negative regulator of PI3K signaling (7). Overexpression of p85α in myotubes reduced insulin-stimulated PI3K/AKT activation (8), and p85α overexpression in mice decreased skeletal muscle insulin signaling (9). Loss of p85α has also been proposed to play a role in cancer. PIK3R1 underexpression was detected in human breast cancer and, in mice, liver-specific *Pik3r1* deletion led to the development of PI3K pathway-activated hepatocellular carcinoma (10, 11).

Here we demonstrate that p85α functions as a tumor suppressor. *PIK3R1* is lost at the genomic and mRNA expression levels in breast cancer. We demonstrate that p85α depletion increases PI3K/AKT signaling and transformation in vitro, and accelerates tumor development in a mouse model of HER2-driven breast cancer. We provide evidence that partial p85α loss increases the ratio of signaling p85–p110 heterodimers bound to activated HER family receptors. Last, we show that p110α-selective inhibition blocks transformation driven by p85α loss. Our results indicate that p85α is a clinically relevant tumor suppressor and suggest that isoform-selective PI3K inhibitors may be effective in the treatment of cancers characterized by p85α expression loss.

Results

***PIK3R1* Expression Is Reduced in Breast Cancers.** To determine whether p85α may play a tumor-suppressive role in breast cancer, we evaluated copy-number loss or mutation of *PIK3R1* in publicly available datasets (12, 13). Such alterations in *PIK3R1* occurred in 23 and 28% of breast cancers, respectively, with the majority of these being hemizygous *PIK3R1* loss (Fig. 1*A*). *PIK3R1* mRNA expression was also significantly reduced by 50 to 77% in breast cancer samples (Fig. 1*B* and Table S1) (14–17). Together, these results indicate that *PIK3R1* is decreased in human breast cancer.

***PIK3R1* Knockdown Transforms Human Mammary Epithelial Cells.** To study whether partial p85α loss transforms in vitro, we used hTERT immortalized human mammary epithelial cells (HMECs) that express a dominant-negative p53 mutant (DDp53). These

Significance

Phosphatidylinositol 3-kinase (PI3K) pathway hyperactivation is a common event in cancer, and understanding alterations in this pathway is critical. Recently, the p85 regulatory subunit of PI3K has come into focus as a novel pathway component targeted in cancers. We find that decreased p85α contributes to transformation of in vitro and in vivo models of breast cancer. We provide evidence that partial loss of p85α increases the binding of p110α–p85 signaling complexes to activated receptors, thereby augmenting PI3K pathway output. Our findings indicate that p85α loss may be transforming in any context where PI3K is activated. Additionally, they implicate a role for monomeric free p85 as a negative regulator of PI3K signaling.

Author contributions: L.M.T., H.C., T.M.R., L.C.C., and J.J.Z. designed research; L.M.T., J.M.S., and C.E.O. performed research; L.M.T., J.M.S., H.C., and L.C.C. contributed new reagents/analytic tools; L.M.T., J.M.S., T.M.R., and J.J.Z. analyzed data; and L.M.T., J.M.S., T.M.R., L.C.C., and J.J.Z. wrote the paper.

Reviewers: J.L., National Cancer Institute; and P.K.V., The Scripps Research Institute.

The authors declare no conflict of interest.

[1]L.M.T. and J.M.S. contributed equally to this work.

[2]To whom correspondence may be addressed. Email: lcantley@med.cornell.edu or jean_zhao@dfci.harvard.edu.

This article contains supporting information online at www.pnas.org/lookup/suppl/doi:10.1073/pnas.1704706114/-/DCSupplemental.

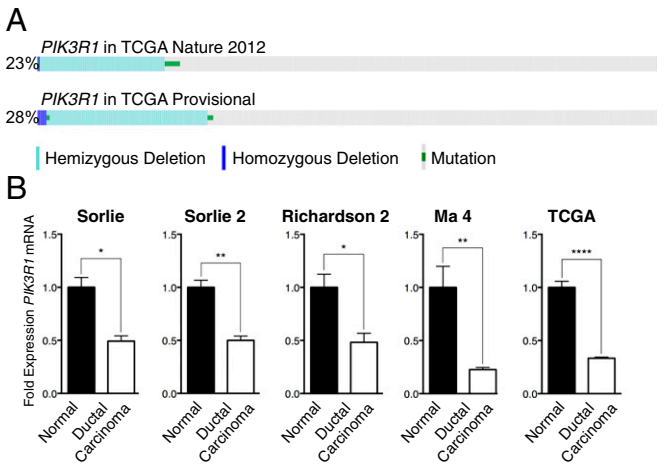

Fig. 1. *PIK3R1* is down-regulated at both the genomic and mRNA expression level in breast cancer. (*A*) The incidence of *PIK3R1* copy-number loss or mutation in TCGA breast cancer cohorts. (*B*) *PIK3R1* expression in breast cancer compared with normal breast (Oncomine). Means ± SEM are shown. $*P < 0.05$, $**P < 0.01$, $****P < 0.0001$; unpaired *t* test.

HMECS are not transformed, as they are unable to form colonies in soft agar. Expression of cancer-associated mutant PIK3CA alleles transforms these cells (18). To address whether decreased *PIK3R1* expression transforms mammary cells, we generated DDp53-HMEC lines with stable *PIK3R1* knockdown. *PIK3R1*-targeted shRNAs reduced p85α expression (Fig. 2*A* and Fig. S1 *A* and *B*). Starvation followed by EGF stimulation increased and sustained PI3K/AKT signaling in *shPIK3R1* cells, as indicated by increased AKT, PRAS40, GSK3β, S6K, and S6 effector phosphorylation (Fig. 2*A*). To assess the functional effect of augmented PI3K/AKT activation in *shPIK3R1* cells, we determined the ability of these cells to undergo anchorage-independent growth. Both *shPIK3R1* lines grow in soft agar (Fig. 2*B*). Expression of *PIK3R1* rescue constructs restores p85α protein levels, attenuates PI3K/AKT pathway activation as indicated by reduced effector phosphorylation (Fig. 2*C* and Fig. S1 *A* and *B*), and partially rescues HMEC transformation mediated by *PIK3R1* knockdown (Fig. 2*D*). Thus, reduction of *PIK3R1* expression activates PI3K/AKT signaling and transforms breast cancer cell lines.

Because the increased signaling in *shPIK3R1* DDp53-HMECs was largely dependent on growth factor stimulation, we investigated whether reduced p85α cooperates with PI3K-activating oncogenes to promote signaling and transformation. We next generated *shPIK3R1* DDp53-HMECs stably expressing neuT, an activated form of HER2/neu. Expression of neuT increases PI3K/AKT activation; concomitant *PIK3R1* knockdown further enhances pathway activation and enhances colony formation, by increasing colony number and size (Fig. 2 *E*–*G*).

Transformation Driven by *PIK3R1* Knockdown Is Mediated by Signaling Through p110α. The PI3K catalytic isoforms play divergent roles in oncogenic signaling, which can inform clinical use of isoform-selective PI3K inhibitors. Accordingly, we used the pan-PI3K inhibitor GDC-0941, the p110α-selective inhibitor BYL-719, and

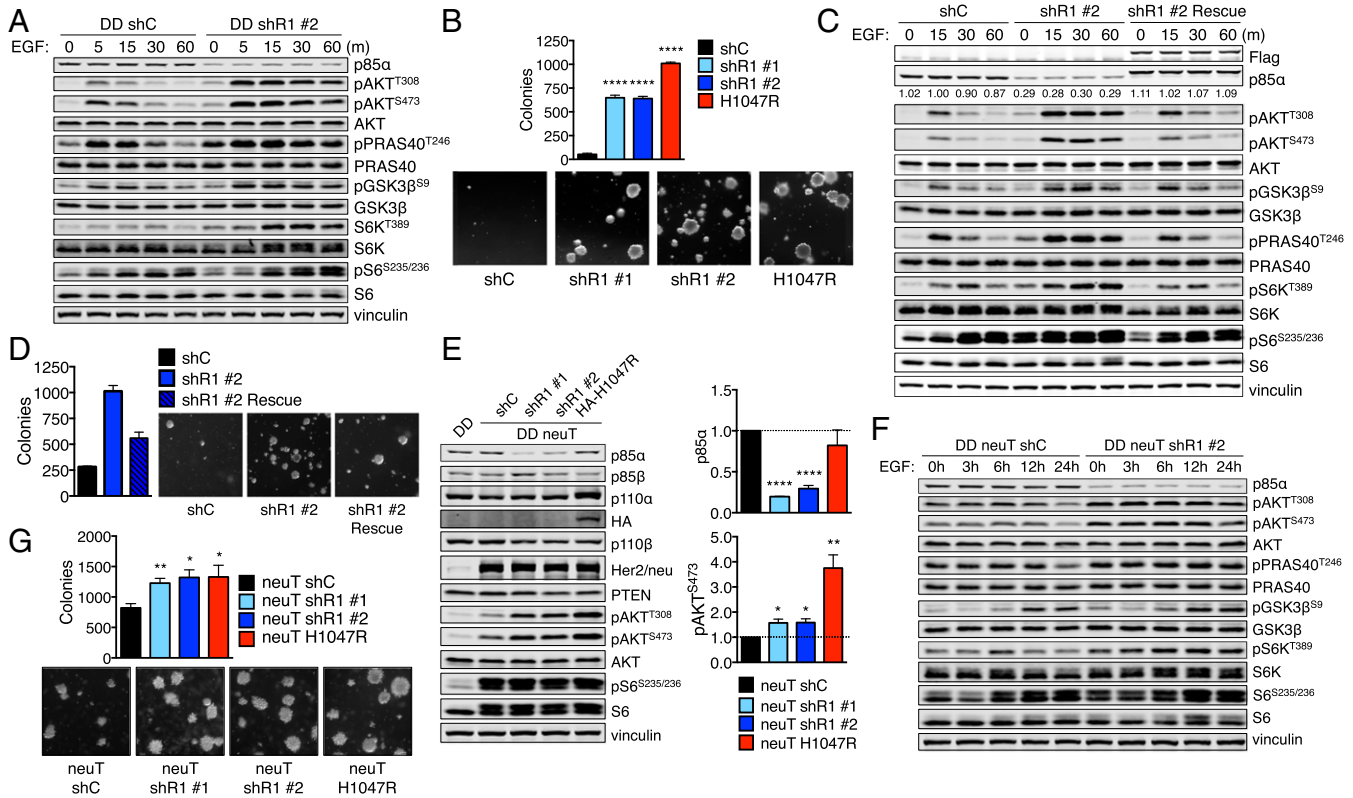

Fig. 2. *PIK3R1* knockdown increases RTK-mediated PI3K/AKT signaling in and transformation of HMECs. (*A*) Control and *shPIK3R1* HMECs were starved and then stimulated with EGF before immunoblotting. (*B*) Cell suspensions of control and *shPIK3R1* HMECs were grown in agar. (*C*) Control, *shPIK3R1*, and rescue HMECs were treated as in *A* before immunoblotting. (*D*) Cell suspensions of control, *shPIK3R1*, and PIK3R1 rescue HMECs were grown in agar. (*E*) Control, *shPIK3R1*, or p110α-H1047R HMECs expressing activated HER2/neu were starved overnight before immunoblotting. (*F*) Control and *shPIK3R1* HER2/neu HMECs were treated as in *A* before immunoblotting. (*G*) Cell suspensions of control and *shPIK3R1* HER2/neu HMECs were grown in agar. Means ± SEM are shown; $n = 3$. $*P < 0.05$, $**P < 0.01$, $****P < 0.0001$; unpaired *t* test.

the p110β-selective inhibitor KIN-193 to determine the contribution of p110 isoforms to the transformation of *shPIK3R1* DDp53-HMECs (3). Treatment with either GDC-0941 or BYL-719, but not KIN-193, effectively blocks colony formation and PI3K/AKT effector signaling in *shPIK3R1* HMECs (Fig. 3 *A*, *B*, and *E*). Thus, transformation with p85α depletion is largely mediated through p110α and not p110β.

Although it has been demonstrated that HER2/neu-driven transformation relies on p110α (19), coexisting genetic events can shift PI3K isoform dependency (20). Therefore, we determined which PI3K catalytic isoform mediates HER2/neu-driven transformation in the context of partial p85α loss. Anchorage-independent growth assays suggest that pan-PI3K or p110α-selective inhibitors block colony formation and attenuate PI3K/AKT effector signaling, whereas p110β-selective inhibition does not (Fig. 3 *C*, *D*, and *F*). Thus, augmented PI3K/AKT signaling in and transformation of *shPIK3R1* HMECs with or without HER2/neu activation are primarily mediated by p110α.

***Pik3r1* Ablation Increases Tumor Formation in Genetically Engineered Mouse Models.** We next used genetically engineered mouse (GEM) models to examine whether loss of p85α contributes to mammary epithelial cell transformation in vivo. Mice bearing a floxed *Pik3r1* allele (21) were crossed with mammary-specific MMTV-Cre mice (22). The resulting MMTV-Cre; $Pik3r1^{+/loxP}$ and MMTV-Cre; $Pik3r1^{loxP/loxP}$ mice have mosaic ablation of one or both *Pik3r1* alleles in luminal mammary epithelial cells, and will hereafter be referred to as MMTV-Cre; $Pik3r1^{+/-}$ and MMTV-Cre; $Pik3r1^{-/-}$, respectively (Fig. S2*A*). *Pik3r1* ablation did not alter mammary gland development throughout pubertal development or lobuloalveolar development during pregnancy (Fig. S2*B*). However, nulliparous MMTV-Cre; $Pik3r1^{+/-}$ and MMTV-Cre; $Pik3r1^{+/-}$ females developed spontaneous mammary tumors with diverse pathology with an average latency of 14.1 mo, average survival of 14.4 mo, and penetrance of 90% (9/10) (Fig. S2*C* and Table S2). Metastasis of the primary tumor to the lung was observed in 11% (1/9) of the mice with spontaneous mammary tumors (Fig. S2*D*). Together, these observations suggest that p85α depletion alone is sufficient for mammary tumor development and metastasis in mice.

To further study the contribution of p85α loss to in vivo mammary tumorigenesis, we combined a GEM model of HER2/neu-driven breast cancer with the conditional *Pik3r1* knockout mice. We bred *Pik3r1* floxed mice with MMTV-NIC mice, which express a bicistronic transgene consisting of an activated HER2/neu allele and Cre recombinase under control of the MMTV LTR promoter (23). The resulting MMTV-NIC; $Pik3r1^{+/-}$ and MMTV-NIC; $Pik3r1^{-/-}$ mice have ablation of one or both *Pik3r1* alleles in the same luminal mammary epithelial cells that express oncogenic HER2/neu. These strains will hereafter be referred to as NIC, NIC; $Pik3r1^{+/-}$, and NIC; $Pik3r1^{-/-}$. NIC, NIC; $Pik3r1^{+/-}$, and NIC; $Pik3r1^{-/-}$ genotypes developed multifocal tumors with 100% penetrance. NIC mice developed palpable tumors with a mean latency of 140 d. Ablation of *Pik3r1* significantly reduced the time to tumor onset: NIC; $Pik3r1^{+/-}$ and NIC; $Pik3r1^{-/-}$ mice

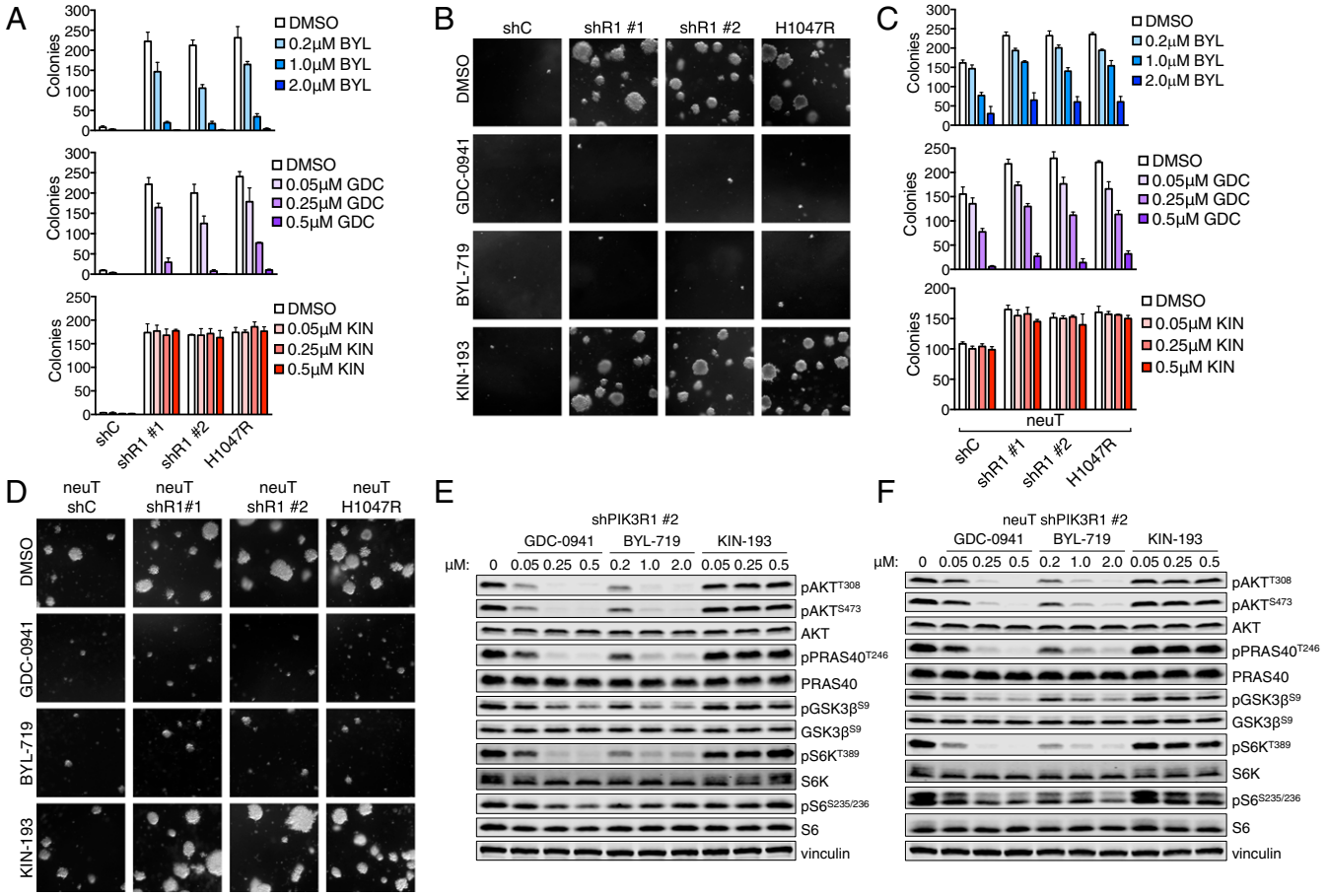

Fig. 3. Transformation of *shPIK3R1* HMECs is blocked by p110α-selective inhibition. (*A*) Cell suspensions of the indicated HMEC lines were grown in agar. (*B*) Images of colonies from the maximum concentration of each condition in *A*. (*C*) Cell suspensions of the indicated HMEC lines were grown in agar. Means ± SD are shown; $n = 3$. (*D*) Images of colonies from the maximum concentration of each treatment condition shown in *C*. (*E*) *shPIK3R1* HMECs were starved, treated for 1 h with the indicated inhibitors, and then stimulated with EGF in the presence of inhibitors before immunoblotting. (*F*) *shPIK3R1* HER2/neu HMECs were treated and processed as in *E*.

developed tumors with mean latencies of 125 and 126 d, respectively (Fig. 4 *A* and *B*). These data indicate that p85α depletion significantly reduces the latency of HER2/neu-driven mammary tumorigenesis in mice.

We examined whether partial p85α loss affected HER2/neu-driven mouse mammary tumors. Tumors from mice of all three genotypes had solid nodular carcinoma histology and tumors of similar weight (Fig. S3 *A* and *B*). A trend toward higher incidence of lung metastasis in mice with *Pik3r1* deletion and an increase in tumor number was observed exclusively in heterozygous NIC; *Pik3r1*$^{+/-}$ mice (Fig. S3 *C* and *D*). However, NIC; *Pik3r1*$^{+/-}$ and NIC; *Pik3r1*$^{-/-}$ tumors had nearly double the proliferation indices (Fig. S3*E*). Together, these results demonstrate that reduced p85α expression increases the proliferative capacity of HER2/neu tumor cells, correlating with the reduced time to mammary tumor onset.

Growth of Mammary Tumors with *Pik3r1* Ablation Is Blocked by p110α-Selective Inhibitors. Because pan-PI3K or p110α-selective inhibitors blocked HMEC transformation driven by partial p85α loss, we determined whether these agents could inhibit growth of HER2/neu-driven mammary tumors with p85α depletion. Primary tumors were excised from a NIC; *Pik3r1*$^{+/-}$ donor female and orthotopically transplanted into NCrNu female recipients. Recipient mice were treated daily with vehicle, GDC-0941, BYL-719, or KIN-193, all without affecting animal body weight (Fig. S3*F*). Treatment with GDC-0941 or BYL-719 significantly reduced tumor growth, whereas KIN-193 had no effect (Fig. 4*C*). Tumors treated with either GDC-0941 or BYL-719 exhibit reduced AKT and S6 phosphorylation, a lower proliferative index, and the presence of TUNEL-positive apoptotic nuclei (Fig. 4 *D* and *E* and Fig. S3*G*). These results indicate that p110α-selective and pan-PI3K inhibitors attenuate PI3K/AKT signaling and block in vivo tumor growth in the context of reduced p85α expression.

***PIK3R1* Knockdown Increases p85–p110α Bound to Activated RTKs.** We next examined the mechanism by which reduced p85α levels could increase PI3K/AKT signaling output and mediate transformation. Despite publications suggesting that p85α may increase PTEN phosphatase activity (24, 25) or PTEN stability (11), we were unable to confirm p85–PTEN association (Fig. S4 *A*–*C*), p85α-mediated reduction in PTEN protein or mRNA levels (Fig. 2*E* and Figs. S1*A* and S4*D*), or p85α-mediated effect on the lipid phosphatase activity of PTEN (Fig. S4 *E* and *F*). *PIK3R1* knockdown also did not affect EGFR phosphorylation, internalization, or degradation (Fig. S5).

However, monomeric, free p85 has been shown to function as a potent p110 inhibitor (7). Activation of RTKs recruits p85–p110 heterodimers to the plasma membrane, which initiates a conformational change to p110α that results in its activation. We therefore considered the possibility that partial p85α loss enhances the specific pool of p85–p110 heterodimers that bind to and potentiate RTK-mediated signal transduction. *PIK3R1* knockdown increases the ratio of p85–p110α heterodimers associated with the RTK ErbB3 (Fig. 5 *A* and *B*). *PIK3R1* knockdown also increases p110α–ErbB3 association, despite a 50% reduction in p85 association with ErbB3 (Fig. 5 *C* and *D*). Increased p85–p110 association with ErbB3 activates AKT (Fig. 5 *E*–*G*). These results demonstrate that partial *PIK3R1* knockdown increases the association of remaining p85 with p110 and ErbB3, promoting oncogenic activation of PI3K/AKT effector signaling.

Discussion

Studies from mouse models with knockout of p85 regulatory subunits have had surprising results. Mice with *Pik3r1* ablation (deleting p85α, p55α, and p50α) (26), just p85α (27), p55α and p50α (28), or *Pik3r2* (deleting p85β) (29) all exhibit hypoglycemia, increased sensitivity to insulin, and augmented insulin-mediated Akt activation. Here we present evidence that *PIK3R1* knockdown transforms HMECs, increasing their proliferation and activation of the PI3K pathway in response to EGF stimulation. We show that in a mouse model of Her2/neu-driven breast cancer, mammary-specific *Pik3r1* ablation reduces the latency of mammary tumor development, increases tumor burden, and up-regulates PI3K pathway activation.

Because p85 stabilizes the p110 subunit and recruits it to the cell membrane (2), it seems paradoxical that a reduction in p85

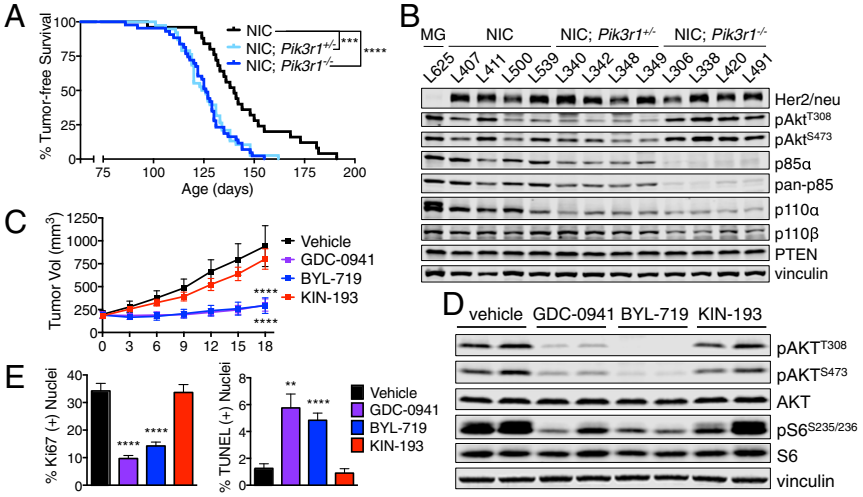

Fig. 4. Tumors characterized by activated Her2/Neu and p85α loss are sensitive to pan-PI3K and p110α-selective inhibition. (*A*) Tumor-free survival of the indicated mouse genotypes. Median tumor-free survival: NIC, 140 d ($n = 25$); NIC; *Pik3r1*$^{+/-}$, 125 d ($n = 38$); NIC; *Pik3r1*$^{-/-}$, 126 d ($n = 43$); log-rank (Mantel–Cox) test. (*B*) Mammary tumor lysates of the indicated genotypes were subjected to immunoblotting. MG, mammary gland from MMTV-Cre mouse genotype. (*C*) Tumor volume of orthotopically transplanted NIC; *Pik3r1*$^{+/-}$ mammary tumors following once-daily treatment with GDC-0941, BYL-719, or KIN-193. Endpoint tumor volumes: vehicle, 942.6 ± 222.9 mm^3; GDC-0941, 199.5 ± 66.8 mm^3; BYL-719, 293.2 ± 85.0 mm^3; KIN-193, 801.6 ± 111.1 mm^3. Means ± SEM are shown; all treatment groups $n \geq 10$; two-way ANOVA with Tukey's multiple-comparisons test. (*D*) Transplanted NIC; *Pik3r1*$^{+/-}$ mammary tumors were treated as in *C*. One hour after treatment on day 4, recipients were killed and tumor tissue was subjected to immunoblotting. (*E*) The percentage of Ki67- or TUNEL-positive nuclei in Fig. S3*G*. Means ± SEM are shown; all groups $n = 8$. $^{**}P < 0.01$, $^{***}P < 0.001$, $^{****}P < 0.0001$; unpaired *t* test.

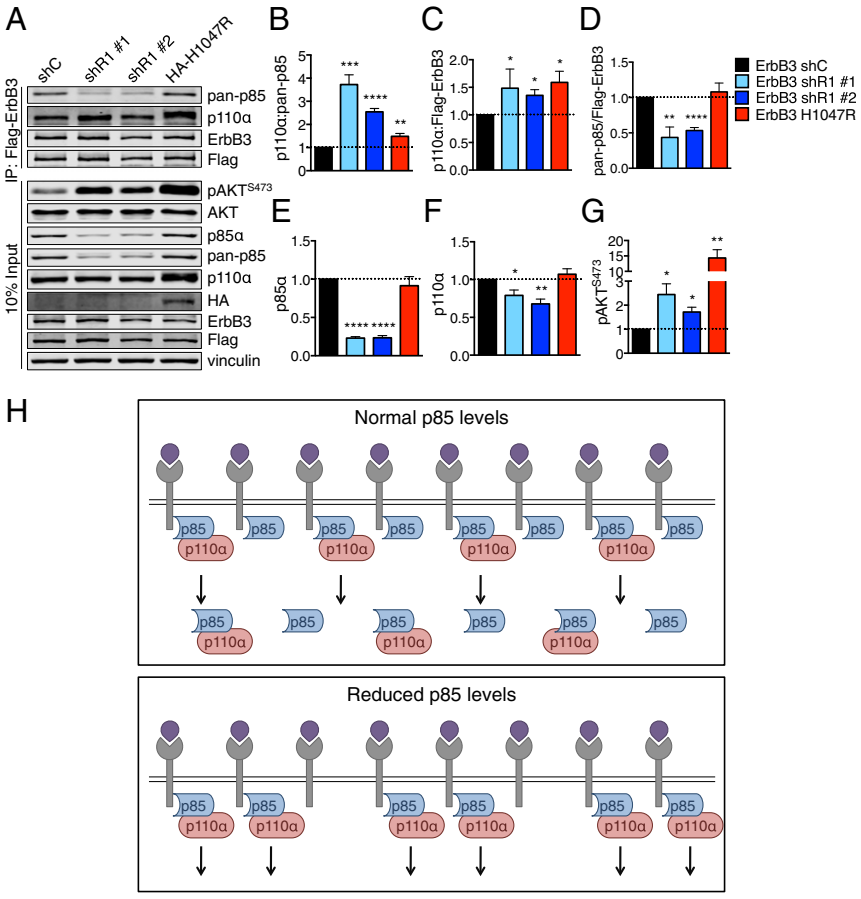

Fig. 5. *PIK3R1* knockdown increases the amount of RTK-bound p110α–p85 in HMECs. (*A*) Control and *shPIK3R1* Flag-ErbB3 HMECs were starved and then lysed. ErbB3 was immunoprecipitated using anti-Flag beads and subjected to immunoblotting. IP, immunoprecipitation. (*B*–*G*) Bands from immunoblots as in *A* were quantified. (*B*–*D*) Quantification of protein levels in ErbB3 IPs. (*B*) Protein levels of p110α were normalized to pan-p85 in IPs, then to the mean for shControl. (*C* and *D*) Protein levels were normalized to ErbB3 in the IPs, then to the mean for shControl. (*E*–*G*) Quantification of protein in inputs. (*E* and *F*) Protein was normalized to vinculin, then to the mean for shControl. (*G*) Protein was normalized to AKT, then to the mean for shControl. Means ± SEM are shown; $n = 4$. $^{*}P < 0.05$, $^{**}P < 0.01$, $^{***}P < 0.001$, $^{****}P < 0.0001$; unpaired *t* test. (*H*) Model in which free p85 competes with p85–p110 to negatively regulate RTK-mediated PI3K/AKT signaling in mammary epithelial cells. (*H*, *Top*) In cells with normal p85α levels, p85 is present in excess of p110. Both free p85 and p85–p110 can compete for binding to activated RTKs, but only p85–p110 can signal. (*H*, *Bottom*) In cells with reduced p85α, the pool of free p85 is selectively depleted. More binding sites on activated RTKs are available for p85–p110, allowing for upregulated PI3K/AKT signaling.

might lead to increased PI3K output. Our data support a model where *PIK3R1* knockdown selectively reduces a pool of free p85α, allowing for increased binding of p85–p110 signaling-capable heterodimers to activated RTKs and increased PI3K output (Fig. 5*H*). Accumulating evidence indicates an imbalance between the regulatory and catalytic PI3K subunits: Immunodepletion suggests that the ratio of p85–p110 dimers to free p85 monomers is 2:1 (6). Quantitative mass spectrometry has shown that endogenous p85 and p110 are present in equal amounts in mouse muscle, liver, fat, and spleen, whereas p85 is present in a twofold excess over p110 in the brain (30). Our data suggest that mammary epithelial cells have p85 in excess of p110, and that this free p85 monomer plays a role in the regulation of PI3K activity. Free p85 can homodimerize, with all four SH2 domains in a flexible conformation. This flexible p85 SH2 conformation (31) is likely to enhance avidity for the nine pYXXM motifs in IRS1 in comparison with the p85–p110 heterodimer, where only the C-terminal p85 SH2 domain has high affinity for the IRS1 motifs (the N-terminal SH2 domain interacts with p110 in a manner that impairs but does not eliminate binding to pYXXM motifs). The clustering and sequestration of IRS1 by the p85 homodimer (32) likely contribute to the ability of free p85 to suppress insulin signaling.

Reports have linked p85α to the control of the activity or stability of PTEN. Mice with liver-specific *Pik3r1* knockout have reduced total PI3K activity but an increase in Akt activation and sustained PIP_3 production; the lipid phosphatase activity of PTEN was found to be reduced (24). Addition of increasing amounts of p85α has also been shown to augment PTEN lipid phosphatase activity in vitro (25). Furthermore, p85α and PTEN have been reported to directly interact (33). We did not find an effect of *PIK3R1* knockdown on the lipid phosphatase activity of PTEN immunoprecipitates in vitro, nor did we detect a reduction in PTEN protein or mRNA in *shPIK3R1* HMECs or in tumors from NIC; *Pik3r1*$^{-/-}$ mice. It may be that PTEN loss is a secondary event, rather than driving transformation mediated by p85α loss.

A number of recent reports have described genomic alterations in *PIK3R1*. Point mutations in the nSH2 and iSH2 p85α domains activate PI3K signaling and promote tumorigenesis in models of glioblastoma (34). Deletion of *PIK3R1* exon 13 was detected in human ovarian and colon cancer cell lines and primary tumors (35). Somatic *PIK3R1* mutations have been found in a variety of cancers with a frequency of 2 to 24% (4, 10). A subset of cancer-associated *PIK3R1* mutations codes for premature truncation of the p85α protein (5), but the transforming mechanism of p85α truncation is unknown. Truncation mutants lose the C-terminal SH2 domain, and thus p85 homodimers with these truncations may not be as effective at binding IRS1. The remaining full-length p85α allele, in cases with hemizygous p85α loss, likely binds more readily to p110α and promotes recruitment to IRS1. Thus, we speculate that truncation mutants that lack the C-terminal SH2 domain might have a similar effect on PI3K signaling as reduction in p85α, and may transform cells by freeing binding spaces on activated RTKs for signaling-proficient p110–p85α heterodimers.

Our data demonstrate that transformation mediated by p85α loss occurs primarily by signaling through p110α. In mice, treatment with pan- and p110α-specific inhibitors slows the growth of transplanted NIC tumors with *Pik3r1* ablation. The data presented here indicate that in cancers where expression of p85α is reduced or functionally inactivated, treatment with p110α-specific inhibitors such as BYL-719 is as effective as pan-PI3K inhibition. Importantly, this is one case where therapeutic targeting of loss

of a tumor suppressor is possible due to identification of activated downstream pathways.

Materials and Methods

For additional information, please refer to *SI Materials and Methods*.

Publicly Available Clinical Data. cBio (www.cbioportal.org) was used to query The Cancer Genome Atlas (TCGA) breast invasive carcinoma studies. The Oncomine database (https://www.oncomine.org) was queried for expression of *PIK3R1* in breast cancer microarray studies. Data were converted to raw expression levels of *PIK3R1* by taking the inverse log2, and then normalized to the mean raw *PIK3R1* expression level of normal breast tissue.

Protein Lysate Preparation, Immunoprecipitation, and Immunoblotting. Cells were lysed in Nonidet P-40 lysis buffer (137 mM NaCl, 20 mM Tris·HCl, pH 8.0, 0.2 mM EDTA, 10% glycerol, 1% Nonidet P-40) with protease and phosphatase inhibitors. For preparation of lysates from tissue, tissue was snap-frozen and then homogenized in Nonidet P-40 lysis buffer using 0.5-mm zirconium oxide beads (Next Advance) in an air-cooling Bullet Blender (Next Advance). For immunoprecipitation of Flag-ErbB3 from HMECs, cells were rinsed with PBS and starved for 4 h before lysis. Anti-Flag beads were incubated with 1 mg lysate, washed, and resuspended in SDS/DTT sample buffer. Proteins were separated by SDS/PAGE and transferred onto nitrocellulose membranes. Proteins of interest were visualized and quantified (Odyssey; LI-COR) after primary antibody incubation: vinculin and Flag (Sigma), pan-p85 and p85α (Millipore), p85β (Santa Cruz), Flag (OriGene), ErbB2 (Calbiochem), and p110α, p110β, HA, ErbB3, PTEN, p-AKT^{T308}, p-AKT^{S473}, total AKT, p-PRAS40^{T246}, PRAS40, p-p70S6K^{T389}, p70S6K, p-GSK3β^{S9}, GSK3β, p-S6$^{S235/236}$, S6, p-EGFR^{Y1068}, and EGFR (Cell Signaling Technology; CST).

Histology and Immunohistochemistry. FFPE tumors were sectioned and mounted. Hematoxylin and eosin staining was performed by the Harvard Medical School Rodent Histopathology Core. Immunohistochemical staining was performed using a sodium citrate antigen retrieval method (Boston BioProducts). Slides were incubated with the following primary antibodies overnight: p85α (EMD Millipore), p-AKT^{S473} (CST), p-S6$^{S235/236}$ (CST), and Ki67 (Vector Labs). Antibody signal was detected using biotinylated goat anti-rabbit IgG secondary antibody and DAB-developed (Vector Labs), and slides were counterstained with hematoxylin (Vector Labs). For TUNEL, the ApopTag Plus Peroxidase In Situ Apoptosis Detection Kit was used (EMD Millipore) followed by a counterstain with methyl green (Vector Labs). Slides were imaged (Nikon; Eclipse E600 microscope).

Growth Factor Stimulation Time-Course Assays. Cells were rinsed with PBS and starved in HMEC starvation medium (DMEM/F12 GlutaMAX with penicillin/streptomycin). Human recombinant EGF was used at 20 ng/mL to stimulate cells.

Anchorage-Independent Growth Assays. Cells were plated in a solution of 0.3% agar in HMEC growth medium on top of a base layer of 0.6% agar in DMEM. Images of unstained colonies were taken (Nikon; SMZ-U). Plates were then stained with 0.5 mg/mL iodonitrotetrazolium chloride (Sigma); pictures of stained plates were taken (Alpha Innotech; AlphaImager EP transilluminator).

Mice. MMTV-Cre (22), NIC (23), and *Pik3r1* floxed (36) mice were backcrossed to FVB/N. Male MMTV-Cre or NIC *Pik3r1*$^{+/-}$ mice were crossed with female *Pik3r1*$^{+/-}$ mice. For orthotopic tumor transplantations, 8-wk-old NCrNu female mice (Harlan) were used. Recipient mice were treated daily with vehicle [0.5% (wt/vol) methylcellulose via oral gavage at 1 mL/kg body weight], BYL-719 (in 0.5% methylcellulose, via oral gavage at 45 mg/kg), GDC-0941 (in 0.5% methylcellulose, via oral gavage at 125 mg/kg), or KIN-193 (in 7.5% 1-methyl-2-pyrrolidinone and 40% PEG400, via i.p. injection at 20 mg/kg). All animals were housed and treated in accordance with protocols approved by the Institutional Animal Care and Use Committees of the Dana-Farber Cancer Institute and Harvard Medical School.

ACKNOWLEDGMENTS. We thank Drs. A. Toker, J. Blenis, and K. Munger and all members of the J.J.Z. laboratory for critical discussions and technical assistance. This study was supported in part by NIH Grants P50 CA168504 (to T.M.R. and J.J.Z.), CA187918-02 (to T.M.R. and J.J.Z.), R35 CA210057 (to J.J.Z.), CA172461 (to J.J.Z.), GM041890 (to L.C.C.), and R35 CA197588 (to L.C.C.), and Breast Cancer Research Foundation (J.J.Z. and L.C.C.).

1. Vanhaesebroeck B, Vogt PK, Rommel C (2010) PI3K: From the bench to the clinic and back. *Curr Top Microbiol Immunol* 347:1–19.
2. Yu J, et al. (1998) Regulation of the p85/p110 phosphatidylinositol 3′-kinase: Stabilization and inhibition of the p110alpha catalytic subunit by the p85 regulatory subunit. *Mol Cell Biol* 18:1379–1387.
3. Thorpe LM, Yuzugullu H, Zhao JJ (2015) PI3K in cancer: Divergent roles of isoforms, modes of activation and therapeutic targeting. *Nat Rev Cancer* 15:7–24.
4. Cheung LW, et al. (2011) High frequency of PIK3R1 and PIK3R2 mutations in endometrial cancer elucidates a novel mechanism for regulation of PTEN protein stability. *Cancer Discov* 1:170–185.
5. Jaiswal BS, et al. (2009) Somatic mutations in p85alpha promote tumorigenesis through class IA PI3K activation. *Cancer Cell* 16:463–474.
6. Mauvais-Jarvis F, et al. (2002) Reduced expression of the murine p85alpha subunit of phosphoinositide 3-kinase improves insulin signaling and ameliorates diabetes. *J Clin Invest* 109:141–149.
7. Luo J, Cantley LC (2005) The negative regulation of phosphoinositide 3-kinase signaling by p85 and its implication in cancer. *Cell Cycle* 4:1309–1312.
8. Ueki K, Algenstaedt P, Mauvais-Jarvis F, Kahn CR (2000) Positive and negative regulation of phosphoinositide 3-kinase-dependent signaling pathways by three different gene products of the p85alpha regulatory subunit. *Mol Cell Biol* 20:8035–8046.
9. Barbour LA, et al. (2005) Increased P85alpha is a potent negative regulator of skeletal muscle insulin signaling and induces in vivo insulin resistance associated with growth hormone excess. *J Biol Chem* 280:37489–37494.
10. Cizkova M, et al. (2013) PIK3R1 underexpression is an independent prognostic marker in breast cancer. *BMC Cancer* 13:545.
11. Taniguchi CM, et al. (2010) The phosphoinositide 3-kinase regulatory subunit p85alpha can exert tumor suppressor properties through negative regulation of growth factor signaling. *Cancer Res* 70:5305–5315.
12. Cancer Genome Atlas Network (2012) Comprehensive molecular portraits of human breast tumours. *Nature* 490:61–70.
13. Cerami E, et al. (2012) The cBio Cancer Genomics Portal: An open platform for exploring multidimensional cancer genomics data. *Cancer Discov* 2:401–404.
14. Sørlie T, et al. (2001) Gene expression patterns of breast carcinomas distinguish tumor subclasses with clinical implications. *Proc Natl Acad Sci USA* 98:10869–10874.
15. Sørlie T, et al. (2003) Repeated observation of breast tumor subtypes in independent gene expression data sets. *Proc Natl Acad Sci USA* 100:8418–8423.
16. Richardson AL, et al. (2006) X chromosomal abnormalities in basal-like human breast cancer. *Cancer Cell* 9:121–132.
17. Ma XJ, Dahiya S, Richardson E, Erlander M, Sgroi DC (2009) Gene expression profiling of the tumor microenvironment during breast cancer progression. *Breast Cancer Res* 11:R7.
18. Zhao JJ, et al. (2005) The oncogenic properties of mutant p110alpha and p110beta phosphatidylinositol 3-kinases in human mammary epithelial cells. *Proc Natl Acad Sci USA* 102:18443–18448.
19. Utermark T, et al. (2012) The p110α and p110β isoforms of PI3K play divergent roles in mammary gland development and tumorigenesis. *Genes Dev* 26:1573–1586.
20. Schmit F, et al. (2014) PI3K isoform dependence of PTEN-deficient tumors can be altered by the genetic context. *Proc Natl Acad Sci USA* 111:6395–6400.
21. Miaczynska M (2013) Effects of membrane trafficking on signaling by receptor tyrosine kinases. *Cold Spring Harb Perspect Biol* 5:a009035.
22. Wagner KU, et al. (1997) Cre-mediated gene deletion in the mammary gland. *Nucleic Acids Res* 25:4323–4330.
23. Ursini-Siegel J, et al. (2008) ShcA signalling is essential for tumour progression in mouse models of human breast cancer. *EMBO J* 27:910–920.
24. Taniguchi CM, et al. (2006) Phosphoinositide 3-kinase regulatory subunit p85alpha suppresses insulin action via positive regulation of PTEN. *Proc Natl Acad Sci USA* 103:12093–12097.
25. Chagpar RB, et al. (2010) Direct positive regulation of PTEN by the p85 subunit of phosphatidylinositol 3-kinase. *Proc Natl Acad Sci USA* 107:5471–5476.
26. Fruman DA, Snapper SB, Yballe CM, Alt FW, Cantley LC (1999) Phosphoinositide 3-kinase knockout mice: Role of p85alpha in B cell development and proliferation. *Biochem Soc Trans* 27:624–629.
27. Terauchi Y, et al. (1999) Increased insulin sensitivity and hypoglycaemia in mice lacking the p85 alpha subunit of phosphoinositide 3-kinase. *Nat Genet* 21:230–235.
28. Chen D, et al. (2004) p50alpha/p55alpha phosphoinositide 3-kinase knockout mice exhibit enhanced insulin sensitivity. *Mol Cell Biol* 24:320–329.
29. Ueki K, et al. (2002) Increased insulin sensitivity in mice lacking p85beta subunit of phosphoinositide 3-kinase. *Proc Natl Acad Sci USA* 99:419–424.
30. Geering B, Cutillas PR, Nock G, Gharbi SI, Vanhaesebroeck B (2007) Class IA phosphoinositide 3-kinases are obligate p85-p110 heterodimers. *Proc Natl Acad Sci USA* 104:7809–7814.
31. LoPiccolo J, et al. (2015) Assembly and molecular architecture of the phosphoinositide 3-kinase p85α homodimer. *J Biol Chem* 290:30390–30405.
32. Luo J, Field SJ, Lee JY, Engelman JA, Cantley LC (2005) The p85 regulatory subunit of phosphoinositide 3-kinase down-regulates IRS-1 signaling via the formation of a sequestration complex. *J Cell Biol* 170:455–464.
33. Rabinovsky R, et al. (2009) p85 associates with unphosphorylated PTEN and the PTEN-associated complex. *Mol Cell Biol* 29:5377–5388.
34. Quayle SN, et al. (2012) Somatic mutations of PIK3R1 promote gliomagenesis. *PLoS One* 7:e49466.
35. Philp AJ, et al. (2001) The phosphatidylinositol 3′-kinase p85alpha gene is an oncogene in human ovarian and colon tumors. *Cancer Res* 61:7426–7429.
36. Luo J, et al. (2005) Class IA phosphoinositide 3-kinase regulates heart size and physiological cardiac hypertrophy. *Mol Cell Biol* 25:9491–9502.